Retrieving Liquid Water Path and Precipitable Water Vapor From the Atmospheric Radiation Measurement (ARM) Microwave Radiometers

David D. Turner, Shepard A. Clough, James C. Liljegren, Eugene E. Clothiaux, Karen E. Cady-Pereira, and Krista L. Gaustad

***Abstract*—Ground-based two-channel microwave radiometers (MWRs) have been used for over 15 years by the Atmospheric Radiation Measurement (ARM) program to provide observations of downwelling emitted radiance from which precipitable water vapor (PWV) and liquid water path (LWP)—two geophysical parameters critical for many areas of atmospheric research—are retrieved. An algorithm that incorporates output from two advanced retrieval techniques, namely, a physical-iterative approach and a computationally efficient statistical method, has been developed to retrieve these parameters. The forward model used in both methods is the monochromatic radiative transfer model MonoRTM. An important component of this MWR RETrieval (MWRRET) algorithm is the determination of small (< 1 K) offsets that are subtracted from the observed brightness temperatures before the retrievals are performed. Accounting for these offsets removes systematic biases from the observations and/or the model spectroscopy necessary for the retrieval, significantly reducing the systematic biases in the retrieved LWP. The MWRRET algorithm significantly provides more accurate retrievals than the original ARM statistical retrieval, which uses monthly retrieval coefficients. By combining the two retrieval methods with the application of brightness temperature offsets to reduce the spurious LWP bias in clear skies, the MWRRET algorithm significantly provides better retrievals of PWV and LWP from the ARM two-channel MWRs compared to the original ARM product.**

***Index Terms*—Meteorology, microwave radiometry, remote sensing.**

I. Introduction

CLOUDS are an important modulator of the radiant energy of the Earth. The treatment of clouds and radiation in global climate models (GCMs) is one of the largest uncertainties in these models [1], and properly modeling the diabatic feedback induced by clouds in GCMs is particularly challenging [2]. Therefore, measurements of both cloud properties and the radiative fluxes are required to improve GCMs and, thus, their prediction of future climate. The collection of a long-term ground-based data set and the subsequent improvement of the treatment of radiation and clouds in GCMs is one of the primary goals of the U.S. Department of Energy's Atmospheric Radiation Measurement (ARM) program [3].

TABLE I
LOCATION OF THE ARM SITES REFERRED TO IN THIS PAPER

Site	Location	Latitude (°N), Longitude (°E), Altitude (m MSL)
SGP C1	Lamont, Oklahoma	36.6, -97.5, 316
NSA C1	Barrow, Alaska	71.3, -156.6, 8
TWP C2	Nauru	-0.5, 166.9, 7
TWP C3	Darwin, Australia	-12.4, 130.9, 30
PYE M1	Point Reyes, California	38.1, -123.0, 24

To first order, the impact of clouds on the radiative flux is dependent on the total amount of condensed water contained in the cloud. Therefore, accurate measurements of the water path, which is defined as the integral of the cloud water content in the vertical column, are critical for accurate modeling of the radiant energy flux. Both shortwave (0.3–4 μm) and longwave (4–100 μm) radiative flux are very sensitive to small errors in the observed liquid water path (LWP), when the LWP is less than 100 g/m^2 (e.g., [4] and [5]). However, a large fraction of the liquid-bearing clouds in the tropics, midlatitudes, and Arctic have LWP less than this threshold ([6]–[8], respectively). As an example, the distribution of LWP in 2004, which was retrieved from ground-based microwave radiometers (MWRs) (Section II) from four ARM sites (Table I) when the colocated laser ceilometer identified a cloud with a base less than 3 km, is shown in Fig. 1. The percentage of the time that the ceilometer-observed cloud had LWP < 100 g/m^2 for this year was 43%, 57%, 61%, and 68% for the SGP C1, TWP C2, TWP C3, and NSA C1 sites, respectively. Therefore, since calculations of the radiative flux are most sensitive for cases with small LWP and clouds with small LWP frequently occur, accurate retrievals of LWP are more critical when the LWP is small.

There are many different techniques available to retrieve LWP from ground-based and space-based remote sensors (e.g., [9]–[11]); however, the most common approach is to retrieve this geophysical parameter from observations in the microwave region of the spectrum (e.g., [12]–[14]). The accuracy of microwave retrievals of LWP, as well as for retrievals that use other

Manuscript received December 21, 2006; revised May 18, 2007. This work was supported by the Environmental Sciences Division, Office of Health and Environmental Research, Office of Energy Research, U.S. Department of Energy.

D. D. Turner is with the Space Science and Engineering Center, University of Wisconsin-Madison, Madison, WI 53706 USA (e-mail: dturner@ssec.wisc.edu).

S. A. Clough and K. E. Cady-Pereira are with Atmospheric and Environmental Research, Inc., Lexington, MA 02421 USA.

J. C. Liljegren is with the Decision and Information Sciences Division, Argonne National Laboratory, Argonne, IL 60439-4814 USA.

E. E. Clothiaux is with the Pennsylvania State University, University Park, PA 16802 USA.

K. L. Gaustad is with the Computational Science and Mathematics Division, Pacific Northwest National Laboratory, Richland, WA 99354 USA.

Digital Object Identifier 10.1109/TGRS.2007.903703

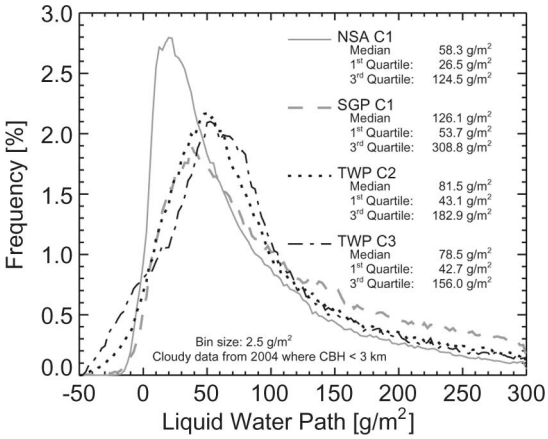

Fig. 1. Frequency distribution of LWP for the year 2004 from four ARM sites, as determined from the MWRs (*stat2* retrieval) when the laser ceilometer identified a cloud with a base below 3 km and the time variation in the 31.4-GHz channel is above a PWV-dependent threshold (see Section III-C). The first, second, and third quartile values are provided for each site. Locations of the ARM sites are provided in Table I.

wavelengths, is dependent upon the calibration and stability of the radiance observation, the accuracy of the forward radiative transfer model, and the accuracy of the inversion approach.

In the microwave region of the spectrum, most liquid hydrometeors fall in the Rayleigh scattering regime (i.e., are very small with respect to the wavelength of the radiation), and thus, the forward radiative transfer models are absorption models and neglect scattering. The relative difference among various microwave absorption models has been extensively investigated (e.g., [7] and [15]–[18]). Differences in the absorption models can lead to biases in the retrieved LWP, but the magnitude of the bias depends on the atmospheric conditions as well as the frequencies used in the retrieval [19].

One way to evaluate the accuracy of LWP retrievals is to investigate the retrieved values in clear-sky conditions when the LWP should be zero [7], [20]. However, even with "perfect" absorption models and inversion techniques, uncertainties in the observations will lead to cases where the LWP is significantly nonzero in clear-sky scenes. This paper presents a methodology that subtracts small offsets from the brightness temperatures observed by a ground-based MWR; removal of these offsets results in a retrieved LWP that is significantly closer to zero in clear-sky scenes. This approach improves the accuracy of LWP, particularly for conditions where the clouds have small LWP, by accounting for small drifts in the instrument's calibration and changes in the atmospheric composition that lead to worse agreement between the true spectroscopy and the model.

It should be noted that others have used clear-sky periods to improve the accuracy of LWP retrievals from MWRs. Liljegren [21] developed a calibration approach that collected tip-curve calibration data during each clear-sky period. van Meijgaard and Crewell [20] identify clear-sky periods and determine the offset that needs to be subtracted to yield zero LWP; this offset is then applied to nearby observations via postprocessing. Our approach (described below) is similar to that of Gaussiat *et al.* [22]; however, they utilize clear-sky periods determined by a lidar to calibrate the measured optical depths, whereas our method adjusts the observed brightness temperatures in clear skies to yield zero LWP.

Precipitable water vapor (PWV), which is the vertical integral of water vapor in the atmospheric column, is also retrieved from MWR observations. Accurate PWV amounts are critical for radiative transfer modeling [23], for specifying the advective forcing for cloud resolving and single column models [24], and evaluation of model humidity fields [25], validation of satellite, geographic positioning system, and other water vapor retrievals [26], and other activities. The ARM program also uses PWV retrieved from MWRs to calibrate the water vapor observations from the operational Raman lidar [27] and collocated radiosondes [28]. Therefore, the absolute accuracy of the PWV is very important and the ARM program strives to improve the retrieval of this quantity. Applying offsets to the observed brightness temperatures impacts the PWV retrievals; the magnitude of the impact will be discussed in Section IV.

Finally, the accuracy of the retrieved geophysical parameters from radiance observations depends on the retrieval methodology used to invert the radiances and the assumptions that are used in the process. We utilize two advanced retrieval approaches to retrieve PWV and LWP from the ARM MWRs. These two retrieval methods, when combined with the "bias offsets" to reduce the spurious LWP in clear skies, significantly provide better retrievals of PWV and LWP from the ARM MWRs relative to the original method.

II. Instrumentation

The ARM program utilizes commercially available ground-based MWRs that sense downwelling radiant energy at 23.8 and 31.4 GHz.[1] Water vapor emission dominates the signal in the 23.8-GHz channel, which is on the wing of the 22.2-GHz water vapor absorption line, whereas liquid water emission constitutes the primary portion of the signal at 31.4 GHz. From these two observations, both PWV and LWP can be retrieved. All retrievals shown here are in the zenith direction.

The calibration of these instruments is maintained by viewing a blackbody target after each sky observation (sky-view observations are collected every 20 s). During the blackbody view, a noise diode is activated which effectively increases the temperature of the blackbody by inserting a nominally fixed amount of additional energy into the system. Therefore, the blackbody view constitutes two points—one at ambient temperature (noise diode off) and one at an elevated temperature (noise diode on)—which allow the gain of the system to be determined. The system gain, together with the observation of the blackbody at a known temperature, is used to convert the observed sky signal into sky brightness temperature. However, accurate calibration requires that the effective temperature of the noise diode be known so that the elevated temperature will also be known. The effective temperature of the noise diode is determined from frequent tip-curve observations [29], whereby the instrument collects observations at a series of angles on

[1]Additional information on the ARM MWRs can be found at the ARM webpage (www.arm.gov/instruments, then select "cloud properties") or at the vendor's website (www.radiometrics.com).

either side of zenith in a vertical plane. The opacity of the atmosphere during such a tip-curve linearly varies with airmass, provided that the atmosphere is horizontally homogeneous, and thus, the gain of the radiometer can be directly determined from the tip-curve observations, which is used to infer the temperature of the noise diode. The ARM MWRs utilize an automated routine that collects tip-curve data whenever the sky is deemed to be clear and homogeneous [21]. This automated routine is able to maintain the calibration of the radiometer to approximately 0.3-K root mean square. However, this uncertainty estimates the random error in the calibration method and does not account for any systematic biases that may be inherent in the method.

III. Algorithm

We have implemented the MWR RETrieval (MWRRET) algorithm in the ARM data system to retrieve PWV and LWP from the MWR observations. There are three components to this algorithm: 1) the forward radiative transfer model used in the retrieval; 2) the two retrieval methodologies; and 3) the removal of the offsets from the observed brightness temperatures.

A. Forward Model

The forward model utilized for both retrieval methods is the monochromatic radiative transfer model MonoRTM developed by Atmospheric and Environmental Research, Inc. [30], [31], which was specifically designed to compute monochromatic radiative transfer, and is particularly useful in the microwave and millimeter-wave spectral regions. The MonoRTM utilizes the same physics as the line-by-line radiative transfer model LBLRTM [32]. In particular, the MonoRTM utilizes a Voigt line shape with all of the parameters provided in the HITRAN line database (e.g., pressure shift coefficient, half-width temperature dependence, and the coefficient for self-broadening and foreign broadening of water vapor) and the continuum model MT_CKD (Mlawer–Tobin–Clough–Kneizys–Davis [31]), which includes foreign- and self-broadened water vapor absorption continua as well as continua for oxygen, nitrogen, carbon dioxide, and ozone. The MonoRTM actually uses a special line file wherein the line strengths for the 22.2- and 183.3-GHz water vapor transitions were determined from laboratory measurements of the Stark effect of the dipole moment [33] and the rest of the parameters are from the HITRAN 2000 database. In particular, the air-broadened half-width of the 22.2-GHz water vapor line utilized by the MonoRTM is the value from the HITRAN database, which was shown by Liljegren *et al.* [34] to be more consistent with multifrequency observations around this water vapor line than the linewidth used in the absorption model of Rosenkranz [16]. Line coupling parameters for oxygen in the microwave region [35] are included in the MonoRTM.[2] Finally, the MonoRTM also includes the liquid water absorption model from Liebe *et al.* [37] and thus is able to compute radiance in scenes with liquid water clouds.

Ascertaining the absolute accuracy of the MonoRTM, or any radiative transfer model for that matter, is a difficult task because it requires accurate atmospheric state measurements (i.e., profiles of water vapor, temperature, and pressure) and accurate radiance observations to use in the closure exercise. The MonoRTM may have uncertainties in the oxygen and the collision-induced nitrogen absorption, both of which are dependent on the temperature and column loading of the dry air (i.e., surface pressure). There are also uncertainties with extrapolating the model to zero PWV due to uncertainties in the water vapor absorption parameters. These uncertainties contribute to a potential bias in the model calculations, which will be grouped with potential biases in the radiometer observations (discussed below).

B. Retrieval Algorithm

The MWR does not directly measure PWV and LWP; these parameters must be retrieved from the observed brightness temperatures, and inadequacies in the retrieval algorithm will result in errors in the retrieved quantities. Historically, the ARM program has utilized a statistical retrieval based in [38]. This method utilized a large historical database of radiosonde profiles and assumed liquid water profiles to compute opacity and mean radiating temperatures at both 23.8 and 31.4 GHz for a wide range of atmospheric conditions. These results were then averaged into monthly coefficients to be used in inverting the observed microwave brightness temperatures [39]. This inversion method, henceforth called *stat1*, is computationally very fast but the retrieved PWV and LWP have significant errors if the current conditions are different from the mean monthly conditions assumed by the retrieval algorithm. Furthermore, this method is location specific, i.e., retrieval coefficients derived at one location may not be applicable to other locations with different elevations (i.e., surface pressure), humidity distributions, atmospheric temperature structure, etc. This method also does not account for the temperature of the cloud, which is a significant uncertainty in the retrieval of LWP due to the temperature dependence of the liquid water emission [37].

To improve the retrieval of LWP, Liljegren *et al.* [12] developed a new statistical method (henceforth called *stat2*) to estimate the instantaneous mean radiating temperature of the atmosphere and the needed retrieval coefficients from surface-based meteorological data. This provides more information to the retrieval algorithm, and the accuracy of the algorithm was improved relative to *stat1*. Furthermore, the use of the surface meteorological data would allow the retrieval to be site independent as long as the initial data set used for developing the statistical relationships included a range of atmospheric state conditions observed in different locations. Additionally, this approach includes estimates of the cloud temperature, derived from a cloud radar (wavelength of 8.6 mm) reflectivity-weighted temperature profile, which further improved the accuracy of the retrieved LWP. In the absence of cloud radar data, the cloud base height from a laser ceilometer is used to estimate the cloud temperature. The regression

[2]In August 2006, the MonoRTM was modified to use the oxygen line parameters from [36]. The analysis shown in this work used the earlier version of MonoRTM.

equations and parameters for the *stat2* retrieval are given in the Appendix.

However, if the atmospheric temperature profile and an estimate of the distribution of water vapor are known (e.g., from a collocated/coincident radiosonde profile), then the most accurate retrieval algorithm is the physical-iterative retrieval method. We utilize the LWP from the *stat2* method as a first guess, and vertically distribute the liquid water according to $\alpha Z^{1/2}$, where Z is the observed radar reflectivity and α is a constant chosen so that the integral of the liquid water equals the first guess LWP. In this physical-iterative approach, the *a priori* information is used in the forward absorption model, and the values of PWV and LWP are iterated until a solution is found such that the difference between the computed and observed brightness temperatures are at a minimum. This approach is more computationally expensive than the *stat2* approach because the forward model is run for each observation. This method, henceforth called "*phys*," is the most accurate method at times when the temperature and water vapor profiles, or atmospheric structure, are known (i.e., observed by the radiosonde); however, for times when the atmospheric structure is not directly observed (such as away from radiosonde launch times), the assumed atmospheric structure (such as from temporally interpolated radiosonde data) may be inaccurate leading to errors in the physically retrieved parameters. The physical retrieval in MWRRET utilizes an optimal estimation framework [40], and the random radiometric uncertainties are propagated to provide uncertainties in the retrieved quantities.

C. T_b Bias Offsets at 23.8 GHz

A systematic bias in the absorption model or the MWR observations translates into a bias in the retrieved products. To reduce any bias in the retrieved PWV, we have developed a technique to determine a brightness temperature T_b offset that is applied to the 23.8-GHz observations before the retrievals are performed. The method requires a large number of observations at radiosonde launch times that are free of liquid water clouds (henceforth called "clear") and that span a significant range of PWV. A large number of cases is required to account for possible bias in radiosonde humidity measurements [28], [41], [42]; this need reduces the temporal frequency at which the T_b offset at 23.8 GHz can be updated. We have elected to yearly compute the 23.8-GHz T_b offset to maintain uniform processing among the different ARM sites with good statistics at each; however, it could be computed twice per year at some sites using the winter-to-summer and summer-to-winter transitions in PWV.

Clear-sky cases were identified by looking at the variability of the 31.4-GHz observations over a 40-min period centered at radiosonde launch time; if the standard deviation is less than $a + b *$ PWV, where $a = 0.15$ K and $b = 0.06$ K/cm, then the sample is assumed to be clear. These coefficients were chosen to provide a simple test to identify scenes that are free of liquid water clouds using only MWR data. For cases identified as free of liquid clouds in 2004 by the above test, a collocated laser ceilometer also indicated it was clear 97%, 78%, 93%, and 95% of the time at the SGP C1, NSA C1, TWP C2, and TWP C3 sites, respectively. The relatively lower level of agreement at the NSA site is due to the occasional presence of ice clouds at low altitudes that are being sensed by the ceilometer, which has a maximum range of approximately 7 km. This simple test allows for the identification of liquid-cloud-free conditions even in the event of failure of the ceilometer.

Since radiosonde humidity measurements may be biased, we iterate to find a single scale factor that is used to scale all radiosonde profiles for a specified period such that the slope of the calculated T_b at 23.8 GHz and the observations is exactly unity. The derivation of this single scale factor assumes that the sensitivity of the MonoRTM calculations at 23.8 GHz to different water vapor burdens is correct. We then compute the T_b bias offset and its uncertainty from the difference of the observations and calculations for cases where the PWV is less than 1.2 cm. This threshold was chosen to minimize the sensitivity of the T_b offset to any nonlinearities in the forward model that may not be correctly accounted for (e.g., self-broadened water vapor continuum absorption); however, the resulting T_b offsets are insensitive of the exact value of this threshold. For sites that do not experience any conditions with PWV < 1.2 cm, such as the ARM site at Nauru in the tropical western Pacific Ocean, no T_b offset is determined for this frequency.

D. T_b Bias Offsets at 31.4 GHz

The uncertainty (i.e., possible dry bias) in the humidity calibration of the radiosonde required us to use a set of clear-sky observations spanning a range of PWV to compute the T_b offset at 23.8 GHz. However, there are still many retrievals in clear skies where the LWP is significantly nonzero regardless of whether the 23.8-GHz T_b offset is applied or not. Therefore, we separately determine a T_b offset for the 31.4-GHz channel for each clear-sky observation that has a coincident radiosonde profile by iterating the physical retrieval until an offset is determined for the 31.4-GHz channel that provides an LWP of zero. To capture any time evolution that might be occurring in the T_b offset, which we are attributing to a time evolution of the calibration for the 31.4-GHz channel, the T_b offset is added to a "rolling database," wherein the oldest T_b offset is removed for each new offset added. The set of offsets in this database is sorted, and the mean of the middle two quartiles, which reduces the impact of any outliers, is subtracted from the observations at 31.4 GHz before the retrieval. In this manner, any spurious cases, potentially affected by clouds that passed the clear-sky screening process, do not significantly impact the retrieved LWP. Clear-sky periods, where the LWP is known to be zero, allows the T_b offset at 31.4 GHz to be updated much more frequently than the 23.8-GHz offset, since the latter requires a large set of radiosondes to account for any potential biases in the calibration of the radiosonde humidity profile.

The number of offsets included in the rolling database is adjustable and is used to strike a balance between reducing the impact of random error in the derived T_b offsets via averaging and introducing a lag effect when the calibration of the channel is quickly changing. Our analysis of the T_b offsets at 31.4 GHz at the SGP C1 site suggests that the 31.4-GHz T_b offset has

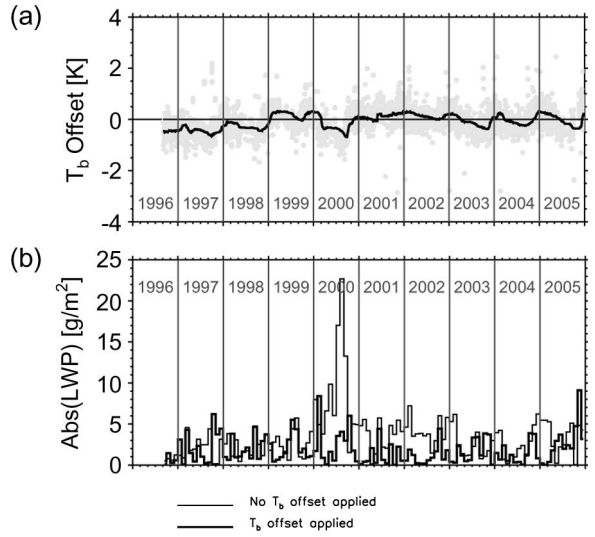

Fig. 2. (a) T_b offsets determined from clear-sky scenes for the (gray points) 31.4-GHz channel of the MWR at the SGP C1 site and the (solid black line) mean of the middle two quartiles that is subtracted from the observations before the retrieval is performed. (b) Absolute value of the median monthly clear-sky LWP from the *stat2* retrieval over the same period of time.

a seasonal dependence (discussed later), and thus, our rolling database includes 100 samples, which is the expected number of clear-sky scenes (i.e., no liquid water clouds overhead) at launch times in a three-month period. The seasonal dependence of this offset at the other ARM sites is considerably smaller than at the Southern Great Plains (SGP) site but the number of liquid-water-free observations at sonde launch times is also smaller due to both local meteorology and the fact that ARM launches fewer radiosondes at the TWP C2 and C3 (nominally two radiosondes per day) and NSA C1 (nominally one radiosonde per day; Monday through Friday) sites. For the TWP and NSA sites, the number of samples in the rolling database is 20. For the ARM mobile facility deployment to Point Reyes, California in 2005 (denoted PYE M1), the number of offsets in the rolling database was set to 30 as nominally four radiosondes per day were launched.

IV. Results

A. T_b Bias Offsets at 31.4 GHz and the Impact on LWP

The T_b offset at 31.4 GHz determined by the above method for the MWR at the SGP C1 facility is shown in Fig. 2. The SGP experiences a wide range of cloud conditions, with frequent clear-sky in all seasons; additionally, typically three to four radiosondes have been launched daily at the SGP C1 site since 1996, and thus, there are many opportunities to compute this T_b offset. The ten-year record of T_b offsets demonstrates both yearly and seasonal variability, with offsets ranging from approximately -0.6 to $+0.4$ K. In 1998, the ARM program transitioned from manual calibration of the MWRs to an automated technique [21]; this may be responsible for the shift in the T_b offsets observed at the SGP at both 23.8 GHz (Table II) and 31.4 GHz (Fig. 2). The T_b offsets at 31.4 GHz from MWRs at other ARM facilities (Fig. 3) also show some variability; however, the differences in cloudiness at the different sites and

TABLE II
Yearly Average Radiosonde Scale Factor [Unitless], T_b Offset at 23.8 GHz and Its 1σ Uncertainty in Parenthesis [K], the Slope Between the Observed and Calculated T_b at 31.8 GHz [K/K] (Using the Indicated Scale Factor), and the Number of Clear-Sky Points Identified for the Period

Site	Year	Scale Factor	T_b Offset at 23.8 GHz	Slope at 31.4 GHz	Number of Points
SGP C1	1996	1.039	-1.13 (0.52)	0.999	220
SGP C1	1997	1.055	-0.83 (0.76)	1.010	438
SGP C1	1998	1.082	-0.79 (0.92)	1.018	340
SGP C1	1999	1.046	0.31 (1.02)	1.022	487
SGP C1	2000	1.072	-0.35 (0.76)	1.043	475
SGP C1	2001	0.977	0.10 (0.72)	0.997	413
SGP C1	2002	1.021	-0.16 (0.59)	1.012	495
SGP C1	2003	1.035	-0.46 (0.50)	1.020	482
SGP C1	2004	0.989	-0.23 (0.57)	1.031	590
SGP C1	2005	0.994	-0.20 (0.61)	1.042	382
PYE M1	2005	1.021	-0.17 (0.98)	1.032	147
NSA C1	2004	1.038	0.32 (0.73)	1.013	53
NSA C1	2005	1.000	0.50 (0.31)	1.011	110
TWP C3	2004	1.103	0.70 (1.00)	0.999	174
TWP C3	2005	1.114	-0.11 (0.40)	1.008	167

The scale factor is the height-independent mean factor that is multiplied to the radiosonde's water vapor mixing ratio profile such that the slope of the observed brightness temperature at 23.8 GHz compared with the MonoRTM computed T_b is exactly 1.000 for all of the clear sky cases within the year. These statistics were not computed for the TWP C2 site in 2004-2005 because the PWV was always much larger than 1.2 cm. The NSA C1 period from 2005 also includes data from Jan – Mar 2006.

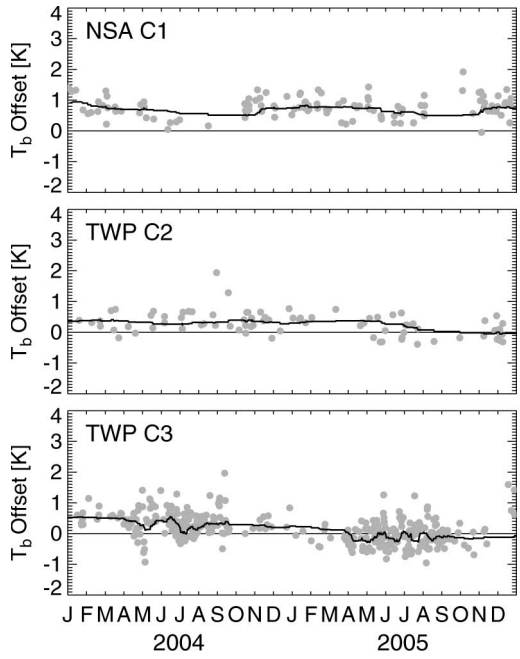

Fig. 3. T_b offsets at 31.4 GHz determined for the NSA C1, TWP C2, and TWP C3 sites for 2004–2005, as in Fig. 2(a).

the lower frequency of radiosonde launches result in fewer clear-sky scenes from which T_b offsets can be computed. This explains the reduction in the number of points relative to the SGP C1 facility.

The sensitivity of T_b to LWP at 31.4 GHz is a function of the amount of PWV (Fig. 4); however, an approximate rule of thumb is that the T_b at 31.4 GHz changes 285 K for an increase of 1 cm of LWP [i.e., the sensitivity is approximately $0.0285\ \mathrm{K}/(\mathrm{g/m^2})$]. Therefore, applying a 0.5-K offset to the

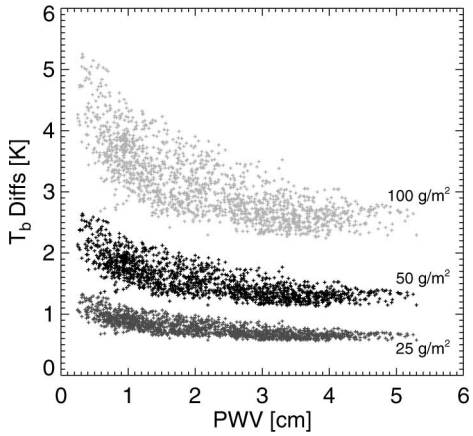

Fig. 4. Cloudy-sky minus clear-sky difference in the brightness temperature at 31.4 GHz for clouds with three different LWPs as a function of PWV, as determined from a series of MonoRTM calculations using 1605 radiosondes launched at the SGP C1 facility in 2004. The different colored points indicate a change in the computed LWP from (medium gray) 0 to 25 g/m^2, (black) 50 g/m^2, and (light gray) 100 g/m^2, respectively.

31.4-GHz observation will change the LWP by approximately 18 g/m^2, which is a substantial amount of liquid water particularly for clouds where the LWP is less than 100 g/m^2. For example, the 31.4-GHz T_b offset at the NSA C1 from January 2004 to March 2006 was always between 0.5 and 1.0 K; if this bias were not removed, then a significant bias would exist in the LWP data set from this period.

Accounting for the bias in the brightness temperature observations and using a more advanced retrieval methodology significantly improve the LWP values. Fig. 5 (top) shows the original *stat1* retrieved LWP during clear-sky scenes over the SGP C1 facility as a function of PWV. Note that there are negative biases in the *stat1* LWP for cases where the PWV is less than 1 cm and for cases when the PWV is between 2.5 and 5 cm; there is also a very large variation in the retrieved clear-sky LWP for the entire PWV range. However, when the *stat2* retrieval is applied using T_b offsets (Fig. 5, middle), the bias is effectively removed for all values of PWV and the spread is significantly decreased. The difference in the retrieved PWV between *stat1* and *stat2* is also significant (Fig. 5, bottom).

B. T_b Bias Offsets at 23.8 GHz and the Impact on PWV

Results from the yearly determination of the T_b offset at 23.8 GHz at several of the ARM sites are shown in Table II. These results demonstrate both site-to-site and temporal variability in the T_b offset at 23.8 GHz. The reason for this variability is most likely instrumental; however, the exact cause is unknown. To put the size of these offsets into perspective, the sensitivity of T_b to PWV at 23.8 GHz is approximately 14 K/cm. Thus, a 1-K T_b offset at this frequency will change the PWV by approximately 0.07 cm. This is a 7% change for PWV at 1 cm and approximately a 2% change for PWV at 4 cm, requiring that the T_b offset at 23.8 GHz be determined and accounted for.

To evaluate the accuracy and sensitivity of the microwave PWV retrievals, a scanning water vapor Raman lidar [43] was scanned toward a 60-m tower that was outfitted with a

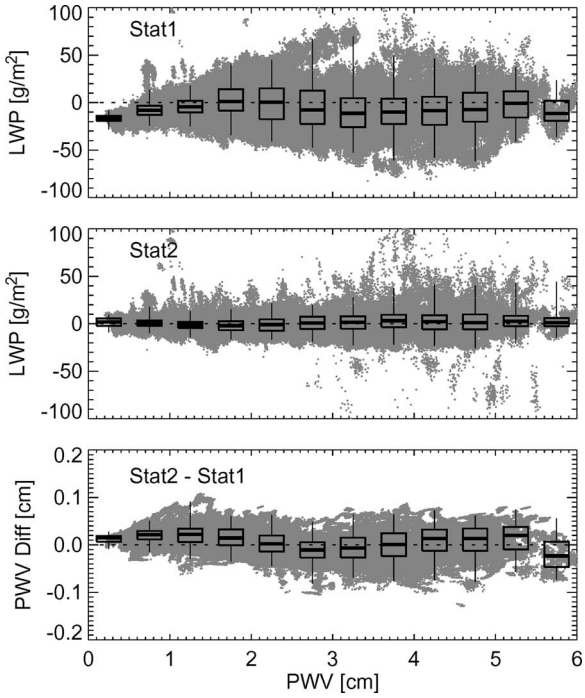

Fig. 5. Distribution of clear-sky LWP from the SGP C1 site from September 1996 to December 2005, computed using the (a) original *stat1* method and the (b) improved *stat2* method with T_b offsets applied. (c) The difference in the retrieved PWV between the two methods is also shown. The box-and-whisker plots show the 25th and 75th percentiles (lower and upper boundaries of the box, respectively), the median value (thick line in the middle of the box), and the ends of the whiskers denote the first and ninety-ninth percentile points in the distribution. The size of each PWV bin is 0.5 cm.

well-characterized chilled mirror water vapor hygrometer [44] during the September 1997 water vapor intensive observation period (WVIOP) [23]. A single height-independent factor is needed to calibrate the Raman lidar's water vapor profile (provided the lidar's near-field overlap correction is correctly specified [45]), and thus, the scanning Raman lidar was calibrated to the chilled mirror observations. This provided an opportunity to compare two well-known calibration standards: the MWR, since the strength of the 22.2-GHz water vapor line is known to better than 1% due to the Stark effect [33] and the chilled mirror hygrometer. This analysis demonstrated an excellent agreement in the sensitivity to water vapor between the two methods with a slope of 0.999 cm/cm and a small offset of 0.109 cm (Fig. 6). [The small differences between the slope and offset reported here versus in Revercomb *et al.* [23] are due to the use of a linear fitting technique that accounts for the uncertainties in both variables, whereas standard linear regression (used in [23]) only accounts for uncertainty in dependent variable.]

The microwave retrievals shown in [23] utilized the *stat1* retrieval method based upon the absorption model of Liebe and Layton [46]. However, the MonoRTM used in MWRRET utilizes a different half-width of the 22.2-GHz water vapor line, a different water vapor continuum, and different treatment of the oxygen absorption. A comparison of the tower-scaled Raman lidar observations with MWRRET's *phys* results also shows excellent agreement in the sensitivity of the microwave retrievals and the chilled mirror calibrated Raman lidar (slope of 1.000 cm/cm), but with a slightly larger offset (0.123 cm).

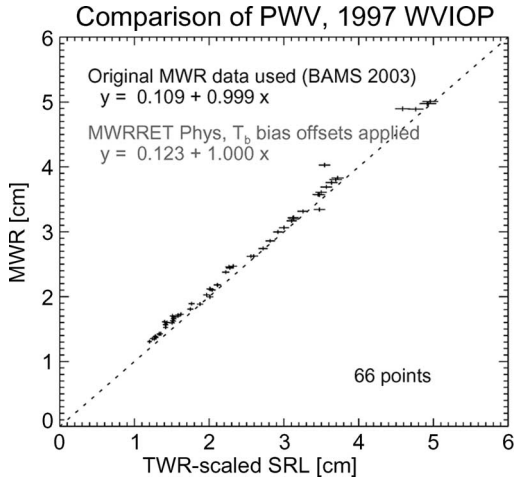

Fig. 6. Comparison of PWV derived from the scanning Raman lidar that was calibrated to a chilled mirror hygrometer on a 60-m tower (x-axis) and the MWR retrievals during clear-sky periods of the 1997 WVIOP. The original data, presented in [23], utilized the absorption model of Liebe and Layton [46] and the *stat1* retrieval method. The same agreement in sensitivity (i.e., a slope of 1.000) is achieved using the MonoRTM absorption model and the physical retrieval in MWRRET. The MWRRET results are not shown here (although the statistics are provided) because they are nearly identical with the original MWR results shown. The correlation coefficient is the same for both comparisons ($r = 0.997$).

The change in the PWV offset in Fig. 6 between the two analyses above is due to the differences between the absorption models and, in particular, the oxygen absorption component [47], as well as the application of the T_b offsets to the MWRRET product. Why is the PWV offset from the MWRRET analysis significantly different than zero if T_b offsets are being applied? One possible explanation is that there are biases in either the chilled mirror hygrometer and/or the Raman lidar (in particular, its overlap correction) that contribute to this bias. Another more likely explanation is that the T_b offset applied to the 23.8-GHz channel only captures an average bias in the radiometric observations over the entire year, and this T_b offset is weighted toward the winter (i.e., low PWV conditions) due to how this T_b bias offset is derived (see Section III-C). Furthermore, this bias likely changes more frequently as demonstrated by the seasonal drift in the T_b bias in the 31.4-GHz channel (Fig. 2). Without an absolute reference water vapor measurement, the T_b bias offset at 23.8 GHz is derived using yearly statistics to get a range of PWV to identify/eliminate any radiosonde dry bias, and thus, the uncertainty in this offset provided in Table II is likely a lower limit, which directly translates into a lower limit on the accuracy of the retrieved PWV.

C. Comparison of Retrieval Techniques

As previously indicated, the physical retrieval is more computationally expensive than the *stat2* method and is thus not practical for operational processing. The physical retrieval at the radiosonde launch time does provide the most accurate retrieval from the MWR observations because the structure of the atmosphere and its mean radiating temperature are specified. However, this is not necessarily the case for MWR observations away from launch times, particularly if the atmospheric structure changes (e.g., during the passage of a frontal boundary). Surface meteorological observations are highly correlated with the atmospheric conditions, which are exploited by the *stat2* method to provide improved retrievals over a more standard statistical retrieval (e.g., *stat1*). For these reasons, we use the *stat2* retrieval to provide LWP and PWV from all the MWR observations, and only run the physical retrieval at radiosonde launch times.

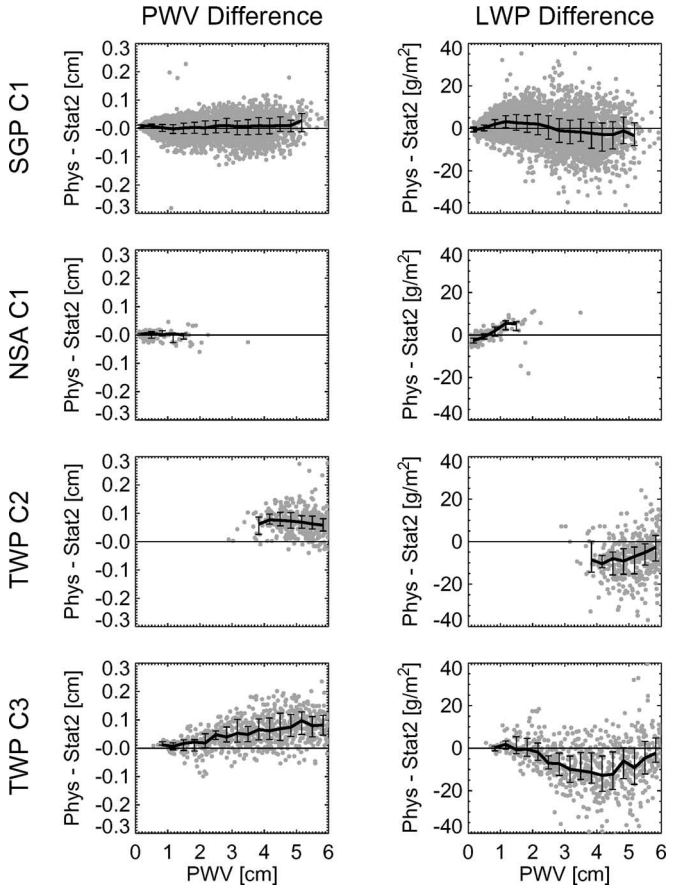

Fig. 7. Differences between the *phys* and *stat2* retrieved values of PWV and LWP in clear-sky scenes as a function of PWV from the SGP C1 (September 1996–January 2005), NSA C1 (January 2004–March 2006), TWP C2 (January 2004–December 2005), and TWP C3 (January 2004–December 2005) sites.

This processing scheme provides ample coincident retrievals to compare the physically retrieved values with the *stat2* results and thus evaluate the adequacy of the regressions used in the *stat2* retrieval. The differences between the *phys* and *stat2* retrieval of both PWV and LWP, as a function of PWV, for all of the clear-sky samples in the indicated years are given in Fig. 7. The results from the SGP, which are virtually identical from year-to-year, demonstrate that the *stat2* retrieval is in good agreement with the physical retrieval over the entire PWV range. However, small differences exist between the two retrieval techniques at the other ARM sites. The NSA site shows no differences between the two methods in PWV, but the *stat2* LWP is too small with the differences between the two retrieval methods increasing as PWV increases. The results from the two tropical sites show that the PWV is underestimated by the *stat2* retrieval by approximately 0.07 cm and that the LWP is overestimated by up to 10 g/m^2 at 4.5 cm of PWV. These

TABLE III
REGRESSION EQUATIONS AND PARAMETERS FOR *stat2* RETRIEVAL ALGORITHM

$T_{mr} = a + b\,T_{sfc} + c\,RH_{sfc} + d\,P_{sfc}$ (1)

$\tau_{dry} = a + b\,(P_{sfc} - e_{sfc})^2 / T_{sfc}$ (2)

$V = a + b\,P_{sfc} + c\,T_{sfc} + d\,T_{sfc}^2 + e\,e_{sfc} + f\,e_{sfc}^2$ (3)

$L = a + b\,P_{sfc} + \exp(c + d\,T_{cld} + e / T_{cld})$ (4)

$L = a + b\,P_{sfc} + c\,P_{sfc}\,e_{sfc} + d\,e_{sfc}^2$ (5)

For equation (1)	a [K]	b [K/K]	c [K]	d [K/hPa]		
$T_{mr,23.8}$	25.6009	0.8160	11.849	7.975e-3		
$T_{mr,31.4}$	14.3028	0.8150	15.008	14.780e-3		
For equation (2)	a [ ]	b [K/bar^2]				
$\tau_{dry,23.8}$	28.1412e-4	3.91636				
$\tau_{dry,31.4}$	39.0804e-4	6.13409				
For equation (3)	a [mm]	b [mm/hPa]	c [mm/K]	d [mm/K^2]	e [mm/hPa]	f [mm/hPa^2]
V_1	573.007	0.083458	-2.92525	0.0050238	0.381837	-0.00544088
$-V_2$	748.769	0.026549	-4.37192	0.00750557	-0.132527	0.00567522
For equation (4)	a [mm]	b [mm/hPa]	c [ ]	d [K^{-1}]	e [K]	
$-L_1$	-0.9522951	0.002082161	-12.02314	0.04446580	0.0	
L_2	1.7023347	0.001636975	22.82242	-0.01826189	-4539.2484	
For equation (5)	a [mm]	b [mm/hPa]	c [mm/hPa^2]	d [mm/hPa^2]		
$-L_1$	-2.36575	0.00400746	0.00010526	-0.0023438		
L_2	-0.52107	0.00534472	0.00031278	-0.0072076		

T_{mr}: mean radiating temperature of the atmosphere [K]; τ_{dry}: the dry opacity of the atmosphere [unitless], V and L: the vapor and liquid retrieval coefficients [mm], respectively; these terms are frequency dependent. T_{sfc}, RH_{sfc}, P_{sfc}, and e_{sfc} are the ambient temperature [K], relative humidity [unitless], barometric pressure [hPa], and vapor pressure [hPa] at the surface, respectively. Equations 3, 4, and 5 have unique coefficients for each frequency: i=1 (23.8 GHz) and i=2 (31.4 GHz).

results demonstrate reasonable accuracy of the *stat2* method over a wide range of atmospheric conditions (Arctic to tropics) and are well within the nominally stated uncertainty of LWP retrieved from these systems of $20-30$ g/m^2 (e.g., [7], [17], and [19]). We have attempted to improve the *stat2* retrievals to further reduce these biases at the different locations but have not yet been successful; however, if the *stat2* retrieval was made location specific (which we have avoided because of the ARM mobile facility), then the biases could be reduced. Fortunately, the differences between the *phys* and *stat2* retrievals are easily parameterized by smooth function, which could then be used to remove the bias from the *stat2* retrievals during postprocessing.

V. CONCLUSION

Radiative transfer model validation, the specification of atmospheric and cloud properties for atmospheric modeling activities (e.g., forcing and evaluating cloud resolving models), studies of the first aerosol indirect effect, and many other areas of atmospheric research require accurate LWP and PWV values. The ARM program has deployed sensitive MWRs, which observe downwelling radiation at 23.8 and 31.4 GHz, at each of its Climate Research Facilities. We have implemented an algorithm called MWRRET that inverts these brightness temperature observations using two advanced retrieval techniques (both based upon the same forward model) to provide retrievals of PWV and LWP. Additionally, to account for systematic biases in the observations as well as possible biases in the absorption model, we have devised methods to determine T_b offsets for both channels that are removed before the retrievals are performed. This results in physically more realistic values of these parameters; for example, the retrieved LWP is much closer to zero in clear skies using this approach than if the T_b offsets were not applied. This new algorithm is a marked improvement over the original ARM retrievals of PWV and LWP from the MWRs.

The 31.4-GHz T_b offsets demonstrate significant seasonal, yearly, and site-to-site variability. Since the model is not changing, we conclude that the majority of this variation is due to (relatively slow) variation in the calibration of the instruments. By accounting for the calibration variability, we are able to maintain more accurate retrievals of PWV and LWP.

The utilization of the two retrieval approaches is very complementary. The physical retrieval provides the most accurate retrievals possible at radiosonde launch times from the MWR; however, it is computationally too expensive to use when processing all of the MWR data. The *stat2* approach uses additional information provided by the surface meteorological measurements in a statistical retrieval, and this method is computationally several orders of magnitude faster than the *phys* method. Comparisons between the two retrieval methods show small but important differences between the two approaches; however, these differences appear to be well behaved, and thus, a site-dependent parameterization of these differences could be used to improve the *stat2* retrieval to provide the same answer as the physical retrieval.

APPENDIX

The *stat2* retrieval utilized in MWRRET is very similar in form to the version published in [12]; however, in an attempt to more closely match the results from the physical retrieval, the formulations were slightly changed. In addition, a different forward model was used in the construction of this statistical

retrieval, which result in updated regression coefficients. The regression equations and parameters used in the *stat2* retrieval are provided in Table III. From these equations, the opacity at each of the microwave frequencies can be computed as

$$\tau = \ln\left(\frac{T_{\rm mr} - T_{\rm cb}}{T_{\rm mr} - T_{\rm sky}}\right) - \tau_{\rm dry} \tag{6}$$

where $T_{\rm cb}$ is the cosmic background (2.75 K), and $T_{\rm sky}$ is the observed sky brightness temperature. The PWV and LWP are then computed as

$$\text{PWV} = V_1\tau_{23} + V_2\tau_{31} \tag{7}$$

$$\text{LWP} = L_1\tau_{23} + L_2\tau_{31} \tag{8}$$

where (4) in Table III is used in the LWP retrieval when the temperature of the cloud is known (from the cloud radar or ceilometer), and (5) in Table III is used when it is not.

ACKNOWLEDGMENT

The authors would like to thank Dr. H. E. Revercomb and Dr. D. C. Tobin for insightful discussions on the retrieval of PWV, and Dr. E. R. Westwater and Dr. R. Marchand for similar discussions on the retrieval of LWP from the ARM MWRs.

REFERENCES

[1] R. D. Cess *et al.*, "Cloud feedback in atmospheric general circulation models: An update," *J. Geophys. Res.*, vol. 101, no. D8, pp. 12 791–12 794, 1996.

[2] J. R. Norris and C. P. Weaver, "Improved techniques for evaluating GCM cloudiness applied to the NCAR CCM3," *J. Clim.*, vol. 14, no. 12, pp. 2540–2551, Jun. 2001.

[3] T. P. Ackerman and G. M. Stokes, "The Atmospheric Radiation Measurement program," *Phys. Today*, vol. 56, pp. 38–45, 2003.

[4] D. D. Turner *et al.*, "Thin liquid water clouds: Their importance and our challenge," *Bull. Amer. Meteorol. Soc.*, vol. 88, no. 2, pp. 177–190, Feb. 2007.

[5] M. Sengupta, E. E. Clothiaux, and T. P. Ackerman, "Climatology of warm boundary layer clouds at the ARM SGP site and their comparison to models," *J. Clim.*, vol. 17, no. 24, pp. 4760–4782, Dec. 2004.

[6] S. A. McFarlane and K. F. Evans, "Clouds and shortwave fluxes at Nauru—Part I: Retrieved cloud properties," *J. Atmos. Sci.*, vol. 61, no. 6, pp. 733–744, Mar. 2004.

[7] R. Marchand, T. Ackerman, E. R. Westwater, S. A. Clough, K. Cady-Pereira, and J. C. Liljegren, "An assessment of microwave absorption models and retrievals of cloud liquid water using clear-sky data," *J. Geophys. Res.*, vol. 108, no. D24, 4773, 2003. DOI:10.1029/2003JD003843.

[8] M. D. Shupe and J. M. Intrieri, "Cloud radiative forcing of the Arctic surface: The influence of cloud properties, surface albedo, and solar zenith angle," *J. Clim.*, vol. 17, no. 3, pp. 616–628, Feb. 2004.

[9] B. Lin and W. B. Rossow, "Observations of cloud liquid water path over oceans: Optical and remote sensing methods," *J. Geophys. Res.*, vol. 99, no. D10, pp. 20 907–20 927, Oct. 1994.

[10] S. Platnick, M. D. King, S. A. Ackerman, W. P. Menzel, B. A. Baum, J. C. Riedi, and R. A. Frey, "The MODIS cloud products: Algorithms and examples from Terra," *IEEE Trans. Geosci. Remote Sens.*, vol. 41, no. 2, pp. 459–473, Feb. 2003.

[11] D. D. Turner, "Arctic mixed-phase cloud properties from AERI-lidar observations: Algorithm and results from SHEBA," *J. Appl. Meteorol.*, vol. 44, no. 4, pp. 427–444, Apr. 2005.

[12] J. C. Liljegren, E. E. Clothiaux, G. G. Mace, S. Kato, and X. Dong, "A new retrieval for cloud liquid water path using a ground-based microwave radiometer and measurements of cloud temperature," *J. Geophys. Res.*, vol. 106, no. D13, pp. 14 485–14 500, Jul. 2001.

[13] U. Löhnert and S. Crewell, "Accuracy of cloud liquid water path from ground-based microwave radiometry—1: Dependency on cloud model statistics," *Radio Sci.*, vol. 38, no. 3, 8041, 2003. DOI:10.1029/2002RS002654.

[14] F. N. Weng, C. Grody, R. Ferraro, A. Basist, and D. Forsth, "Cloud liquid water climatology from the Special Sensor Microwave/Imager," *J. Clim.*, vol. 10, no. 5, pp. 1086–1098, May 1997.

[15] Y. Han, J. B. Snider, E. R. Westwater, S. H. Melfi, and R. A. Ferrare, "Observations of water vapor by ground-based microwave radiometers and Raman lidar," *J. Geophys. Res.*, vol. 99, no. D9, pp. 18 695–18 702, 1994.

[16] P. W. Rosenkranz, "Water vapor continuum absorption: A comparison of measurements and models," *Radio Sci.*, vol. 33, pp. 919–928, 1998.

[17] E. R. Westwater, Y. Han, M. D. Shupe, and S. Matrosov, "Analysis of integrated cloud liquid and precipitable water vapor retrievals from microwave radiometers during the Surface Heat Budget of the Arctic Ocean project," *J. Geophys. Res.*, vol. 106, no. D23, pp. 32 019–32 030, 2001.

[18] T. Hewison, D. Cimini, L. Martin, C. Gaffard, and J. Nash, "Validating clear air absorption models using ground-based microwave radiometers and vice-versa," *Meteorol. Z.*, vol. 15, no. 1, pp. 27–36, 2006. DOI:10.1127/0941-2948/2006/0097.

[19] S. Crewell and U. Löhnert, "Accuracy of cloud liquid water path from ground-based microwave radiometry—2: Sensor accuracy and synergy," *Radio Sci.*, vol. 38, no. 3, 8042, Feb. 2003. DOI:10.1029/2002RS002634.

[20] E. van Meijgaard and S. Crewell, "Comparison of model-predicted liquid water path with ground-based measurements during CLIWA-NET," *Atmos. Res.*, vol. 75, no. 3, pp. 226–2001, May 2005.

[21] J. C. Liljegren, "Automatic self-calibration of ARM microwave radiometers," in *Microwave Radiometry and Remote Sensing of the Earth's Surface and Atmosphere*, P. Pampaloni and S. Paloscia, Eds. Utrecht, The Netherlands: VSP Press, 2000, pp. 433–443.

[22] N. Gaussiat, R. J. Hogan, and A. J. Illingworth, "Accurate liquid water path retrieval from low-cost microwave radiometers using additional information from a lidar ceilometer and operational forecast models," *J. Atmos. Ocean. Technol.*, vol. 24, pp. 1562–1575, 2007. DOI:10.1175/JTECH2053.1.

[23] H. E. Revercomb *et al.*, "The ARM program's water vapor intensive observation periods: Overview, initial accomplishments, and future challenges," *Bull. Amer. Meteorol. Soc.*, vol. 84, no. 2, pp. 217–236, Feb. 2003.

[24] M. H. Zhang and J. L. Lin, "Constrained variational analysis of sounding data based on column-integrated budgets of mass, heat, moisture, and momentum: Approach and application to ARM measurements," *J. Atmos. Sci.*, vol. 54, no. 11, pp. 1503–1524, Jun. 1997.

[25] A. Memmo, E. Fionda, T. Paolucci, D. Cimini, R. Ferretti, S. Bonafoni, and P. Ciotti, "Comparison of MM5 integrated water vapor with microwave radiometer, GPS, and radiosonde measurements," *IEEE Trans. Geosci. Remote Sens.*, vol. 43, no. 5, pp. 1050–1058, May 2005.

[26] V. Mattioli, E. R. Westwater, and V. R. Morris, "Forward model studies of water vapor using scanning microwave radiometers, global positioning system, and radiosondes during the cloudiness intercomparison experiment," *IEEE Trans. Geosci. Remote Sens.*, vol. 43, no. 5, pp. 1012–1021, May 2005.

[27] D. D. Turner and J. E. M. Goldsmith, "Twenty-four-hour Raman lidar water vapor measurements during the Atmospheric Radiation Measurement Program's 1996 and 1997 water vapor intensive observation periods," *J. Atmos. Ocean. Technol.*, vol. 16, no. 8, pp. 1062–1076, Aug. 1999.

[28] D. D. Turner, B. M. Lesht, S. A. Clough, J. C. Liljegren, H. E. Revercomb, and D. C. Tobin, "Dry bias and variability in Vaisala RS80-H Radiosondes: The ARM experience," *J. Atmos. Ocean. Technol.*, vol. 20, no. 1, pp. 117–132, Jan. 2003.

[29] Y. Han and E. R. Westwater, "Analysis and improvement of tipping calibration for ground-based microwave radiometers," *IEEE Trans. Geosci. Remote Sens.*, vol. 38, no. 3, pp. 43–52, May 2000.

[30] S. A. Boukabara, S. A. Clough, and R. N. Hoffman, "MonoRTM: A monochromatic radiative transfer model for microwave and laser calculation," presented at the Specialist Meeting Microwave Remote Sensing, Boulder, CO, 2001.

[31] S. A. Clough, M. W. Shephard, E. J. Mlawer, J. S. Delamere, M. J. Iacono, K. Cady-Pereira, S. Boukabara, and P. D. Brown, "Atmospheric radiative transfer modeling: A summary of the AER codes," *J. Quant. Spectrosc. Radiat. Transf.*, vol. 91, no. 2, pp. 233–244, Mar. 2005.

[32] S. A. Clough, M. J. Iacono, and J.-L. Moncet, "Line-by-line calculation of atmospheric fluxes and cooling rates: Application to water vapor," *J. Geophys. Res.*, vol. 97, no. D14, pp. 15 761–15 781, 1992.

[33] S. A. Clough, Y. Beers, G. P. Klein, and L. S. Rothman, "Dipole moment of water vapor from Stark measurements of H_2O, HDO, and D_2O," *J. Chem. Phys.*, vol. 59, no. 5, pp. 2254–2259, Sep. 1973.

[34] J. C. Liljegren, S. A. Boukabara, K. Cady-Pereira, and S. A. Clough, "The effect of the half-width of the 22-GHz water vapor line on retrievals of temperature and water vapor profiles with a 12-channel microwave radiometer," *IEEE Trans. Geosci. Remote Sens.*, vol. 43, no. 5, pp. 1102–1108, May 2005.
[35] M. L. Hoke, S. A. Clough, W. J. Lafferty, and B. W. Olson, "Line coupling in oxygen and carbon dioxide," in *Proc. IRS 88: Current Problems in Atmospheric Radiation*, J. Lenoble and J. F. Geleyn, Eds., Hampton, VA, 1989, pp. 368–371.
[36] M. Y. Tretyakov, M. A. Koshelev, V. V. Dorovshikh, D. S. Makarov, and P. W. Rosenkranz, "60-GHz oxygen band: Precise broadening and central frequencies of fine-structure lines, absolute absorption profile at atmospheric pressure, and revision of mixing-coefficients," *J. Mol. Spectrosc.*, vol. 231, no. 1, pp. 1–14, May 2005.
[37] H. J. Liebe, G. A. Hufford, and T. Manabe, "A model for the complex permittivity of water at frequencies below 1 THz," *Int. J. Infrared Millim. Waves*, vol. 12, no. 7, pp. 659–675, Jul. 1991.
[38] E. R. Westwater, "Ground-based microwave remote sensing of meteorological variables," in *Atmospheric Remote Sensing by Microwave Radiometry*, M. A. Jensen, Ed. New York: Wiley, 1993, pp. 145–213.
[39] J. C. Liljegren and B. M. Lesht, "Measurements of integrated water vapor and cloud liquid water from microwave radiometers at the DOE ARM cloud and radiation testbed in the U.S. Southern Great Plains," in *Proc. IGARSS*, Lincoln, NE, 1996, pp. 1675–1677.
[40] C. D. Rodgers, *Inverse Methods for Atmospheric Sounding: Theory and Practice*. Singapore: World Scientific, 2000.
[41] J. Wang, H. L. Cole, D. J. Carlson, E. R. Miller, K. Beierle, A. Paukkunen, and T. K. Laine, "Corrections of humidity measurement errors from the Vaisala RS80 radiosonde—Application to TOGA COARE data," *J. Atmos. Ocean. Technol.*, vol. 19, no. 7, pp. 981–1002, Jul. 2002.
[42] K. E. Cady-Pereira, M. W. Shephard, D. D. Turner, E. J. Mlawer, S. A. Clough, and T. J. Wagner, "Improved total column precipitable water vapor from Vaisala RS90 and RS92 radiosonde humidity sensors," *J. Atmos. Ocean. Technol.*, 2007, submitted for publication.
[43] D. N. Whiteman *et al.*, "Raman lidar measurements of water vapor and cirrus clouds during the passage of hurricane Bonnie," *J. Geophys. Res.*, vol. 106, no. D6, pp. 5211–5225, Mar. 2000.
[44] S. J. Richardson, M. E. Splitt, and B. M. Lesht, "Enhancement of ARM surface meteorological observations during the fall 1996 water vapor intensive observation period," *J. Atmos. Ocean. Technol.*, vol. 17, no. 3, pp. 312–322, Mar. 2000.
[45] D. N. Whiteman, S. H. Melfi, and R. A. Ferrare, "Raman lidar system for measurement of water vapor and aerosols in the Earth's atmosphere," *Appl. Opt.*, vol. 31, no. 16, pp. 3068–3082, Jun. 1992.
[46] H. J. Liebe and D. H. Layton, "Millimeter wave properties of the atmosphere: Laboratory studies and propagation modeling," Nat. Telecommun. and Inf. Admin (NTIA), Boulder, CO, Rep. 87-24, 1987.
[47] M. P. Cadeddu, V. Payne, S. A. Clough, K. Cady-Periera, and J. C. Liljegren, "Effect of the oxygen line-parameter modeling on temperature and humidity retrievals from ground-based microwave radiometers," *IEEE Trans. Geosci. Remote Sens.*, vol. 45, no. 7, pp. 2216–2223, Jul. 2006.

David D. Turner received the B.A. and M.S. degrees in mathematics from Eastern Washington University, Cheney, in 1992 and 1994, respectively, and the Ph.D. degree in atmospheric science from the University of Wisconsin, Madison, in 2003.

He is currently a Researcher with the Space Science and Engineering Center, University of Wisconsin. He is actively involved in the Department of Energy's Atmospheric Radiation Measurement (ARM) program, and is currently the Chair of the ARM Radiative Processes working group and is a member of the ARM Science Team Executive Committee. His current research interests include infrared and microwave remote sensing, longwave radiative transfer, and retrieving water vapor and aerosol properties from active and passive remote sensors.

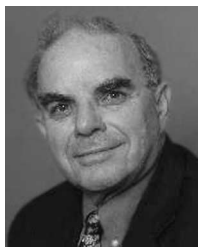

Shepard A. Clough received the B.E. degree in physics from Cornell University, Ithaca, NY, in 1954 and the M.A. degree in physics from Columbia University, New York, in 1958.

He is a member of the ARM Science Team and is a participant in the Earth Observing System (EOS) as a Coinvestigator on the Tropospheric Emission Spectrometer, a high-resolution spectrometer launched on the EOS AURA mission. He has been responsible for the development of the widely used atmospheric radiative modeling codes including LBLRTM, RRTM, and CHARTS. He has made significant contributions to the HITRAN spectroscopic database. He is currently with Atmospheric and Environmental Research, Inc., Lexington, MA. His current research interests include atmospheric radiative transfer, molecular physics, and approaches to the retrieval of information from remotely sensed measurements. His current activities are focused on the improvement of radiative transfer modeling for general circulation models with application to climate change studies.

Mr. Clough is currently a member of the International Radiation Commission.

James. C. Liljegren received the B.S., M.S., and Ph.D. degrees in mechanical engineering from the University of Illinois, Urbana-Champaign. His doctoral dissertation was on the development and field validation of a stochastic model of turbulent dispersion in the convective boundary layer.

He is an Atmospheric Scientist with the Decision and Information Sciences Division, Argonne National Laboratory, Argonne, IL. His research efforts have included developing continuous autonomous calibration algorithms for ARM microwave radiometers, developing improved retrieval algorithms for precipitable water, cloud liquid water path, and vertical profiles of temperature and humidity, and refining the microwave spectroscopy underlying the retrievals. He has been involved in the ARM program, since its inception in 1990, in science team and infrastructure roles. He has participated in field campaigns at the ARM Southern Great Plains and North Slope of Alaska sites focused on water vapor measurements, including an extended comparison of slant water measurements with GPS and microwave radiometers. He also participated in the Surface Heat Budget of the Arctic (SHEBA) campaign. His current research interests include atmospheric remote sensing, primarily using passive microwave radiometry.

Eugene E. Clothiaux received the B.Sc. degree in physics from Auburn University, Auburn, AL, in 1983 and the M.S. and Ph.D. degrees from Brown University, Providence, RI, in 1986 and 1990, respectively, both in physics.

In 1991, he was awarded a Department of Energy Global Change Distinguished Postdoctoral Fellowship to study radar returns from clear-air turbulence and clouds using a number of different radars developed at the Pennsylvania State University, University Park, where he is currently an Associate Professor. His research interests include ground- and satellite-based remote sensing of clouds with an emphasis on trying to understand the impact of clouds on the radiation budget of the Earth.

Karen E. Cady-Pereira received the B.S. degree in physics from the University of São Paulo, São Paulo, Brazil and the M.S. degree in civil engineering from the Massachusetts Institute of Technology, Cambridge.

She is currently with Atmospheric and Environmental Research, Inc., Lexington, MA, where she has worked on radiative transfer problems in the visible, infrared, and microwave. Her current interest is on the retrieval of trace gases in the atmosphere. Recently, she has also extensively worked on modeling scattering by aerosols, clouds, and icy surfaces.

Krista L. Gaustad received the B.S.E.E. and M.S. degrees in electrical engineering from Auburn University, Auburn, AL, in 1988 and 1991, respectively.

She is currently a Senior Research Engineer with the Computational Science and Mathematics Division, Pacific Northwest National Laboratory, Richland, WA, where she develops, implements, and tests data management and science algorithms used to process, assess, and analyze data collected from ARM's instrument sites.